Psychophysiology

WILEY

PSYCHOPHYSIOLOGY SPR

ORIGINAL ARTICLE OPEN ACCESS

Reactivity of the Autonomic Nervous System During Visual-Physical Incongruent Walking Conditions—A Virtual Reality Study

Adi Lustig[1,2] | Amit Benady[1,3,4,5] | Sharon Gilaie-Dotan[3,6] | Meir Plotnik[1,2,7]

[1]Center of Advanced Technologies in Rehabilitation, Sheba Medical Center, Tel HaShomer, Israel | [2]Department of Physiology and Pharmacology, Faculty of Medicine, Tel Aviv University, Tel Aviv-Yafo, Israel | [3]School of Optometry and Vision Science, Faculty of Life Sciences, Bar-Ilan University, Ramat Gan, Israel | [4]Orthopedic Department, Tel Aviv Sourasky Medical Center, Tel Aviv, Israel | [5]Department of Anatomy and Anthropology, Faculty of Medicine, Tel Aviv University, Tel Aviv, Israel | [6]The Gonda Multidisciplinary Brain Research Center, Bar-Ilan University, Ramat-Gan, Israel | [7]Sagol School of Neuroscience, Tel Aviv University, Tel Aviv, Israel

Correspondence: Meir Plotnik (Meir.PlotnikPeleg@sheba.health.gov.il)

Received: 8 December 2024 | **Revised:** 10 April 2025 | **Accepted:** 24 April 2025

Funding: The authors received no specific funding for this work.

Keywords: affect | heart rate | heart rate variability | motor control | perception | psychophysics

ABSTRACT

The force of gravity critically impacts locomotion regulation while walking on inclined surfaces. To construct an updated assessment about the gravitational consequences and change gait patterns accordingly, the central nervous system (CNS) integrates multiple sensorial cues, including vestibular and proprioceptive (i.e., body-based cues) and visual. Not much is known about the contribution of the autonomic nervous system (ANS) to locomotion regulation, especially when multiple types of sensorial cues are involved. Here we examine the responsiveness of the ANS, as reflected by cardiac reactivity, for example heart rate (HR) and heart rate variability (HRV), to coherent versus non-coherent sensorimotor signaling. Fourteen healthy young participants completed level, uphill, and downhill self-paced walking trials in a virtual reality (VR) environment in which the incline of the visual scene was either congruent or incongruent with the physical incline of the walking surface. We found that during level walking, incongruent visual cues (i.e., up/downhill scenery) triggered alterations in ANS balance, reflected in HRV decrease and in a residual increase of HR. Taken together with the fact that an ultimate change in gait patterns requires alterations in cardiac resources, we speculate that ANS function and its responsive modes of action are, in fact, facilitating adaptive behavior.

1 | Introduction

1.1 | Gait Modulations During Walking on Inclined Surfaces

Functional locomotion on inclined surfaces is subjected to gravitational forces, which change the spatial perspective, postural equilibrium, power demands, and consequently, the required movement production of the walker (Lacquaniti et al. 2014; Cavagna et al. 2000). Downhill walking (when gravitational acceleration aligns with the propulsion generated by walking) and uphill walking (when the gravitational acceleration is acting in the opposite direction of walking) are critically impacted by the force of gravity (Kimel-Naor et al. 2017). To maintain postural stability in these circumstances, locomotion control relies on an 'internal model of gravity (IMG)' that enables the accommodation of behavior to the consequential effects of gravity (Lacquaniti et al. 2014; Balestrucci et al. 2017). The central nervous system (CNS) addresses multiple sensory cues, including vestibular and proprioceptive (known together as body-based

cues), and visual cues, which are being integrated across time and in a differentially weighted manner to construct an updated percept of the gravity-related environmental state. This multisensory information is being assessed against accumulated experience and prior practice to generate adequate gait modulations in accordance with the updated precept (Lacquaniti et al. 2014; Balestrucci et al. 2017; Campos et al. 2014; Larra et al. 2020).

The initial reaction to a destabilizing environmental change in locomotion regulation was explained by the *indirect prediction* model (O'Connor and Donelan 2012; Pearson 2004; Cano Porras et al. 2020) which relies mostly on prior experience. This model suggests that neural constructs controlling locomotion promptly trigger pre-programmed gait patterns following destabilizing events, which are detected by fast perceived cues (i.e., visual) (Cano Porras et al. 2020; Lacquaniti et al. 2015; O'Connor and Donelan 2012). The *predictive coding* concept posits that these initial visually induced changes in gait patterns are the consequences of model-dependent top-down behavior regulation (Owens, Friston, et al. 2018; Dobrushina et al. 2021). Hence, during downhill walking, downhill visual cues activate the '*braking* effect' in anticipation of gravity-related acceleration, and during uphill walking, uphill visual cues promote an '*exertion* effect' in anticipation of gravity-related deceleration (Cano Porras et al. 2020), which is accompanied by an increase in metabolic cost (Minetti et al. 2002).

The descending (i.e., top-down) prediction is being constantly compared against new incoming sensory inputs (i.e., stimulus-dependent bottom-up evidence set) in a prediction error method (Skaggs 2023; Huang and Rao 2011). An iterative recalibration process of the relative influence of all sensorial cues (intended to minimize the prediction error) leads to a gradual re-stabilization of walking patterns, also known as *sensory reweighting* (Campos et al. 2014; O'Connor and Donelan 2012; Assländer and Peterka 2016). This functional architecture allows the system to engage adaptive behavior by balancing between priors and external stimuli in order to maintain postural stability (Owens, Friston, et al. 2018; Owens, Allen, et al. 2018; Thayer et al. 2012).

1.2 | The Role of the Autonomic Nervous System

All communications between the CNS that is where plans are initiated and re-evaluated, and the body that is the executing effectors, are mediated also through the autonomic nervous system (ANS) (Critchley and Garfinkel 2015). ANS function is known to be involved both in bottom-up signaling ascending the neuro-axis, that is conveying 'somatic feedback' to the CNS (Critchley and Garfinkel 2015; De Kloet et al. 1999; Critchley and Harrison 2013), and in the top-down brain signaling influencing autonomic response through efferent autonomic output (Owens 2020). However, while ANS modulations are clearly involved in the process of modulating gait patterns (e.g., heart rate—gait speed relation), the mechanisms by which ANS contributes to locomotion regulation are not fully understood.

The most frequently used measure of ANS activity is heart rate (HR), which is antagonistically controlled by the sympathetic and parasympathetic branches of the ANS (Hagemann et al. 2003) as follows: At rest, parasympathetic inhibitory effects predominate, reducing HR. Early demands for metabolic resources (e.g., with an increase in physical activity) initiate the removal of the parasympathetic inhibition, which enables a gradual increase in HR. As physical stress proceeds, sympathetic stimulation elevates to accelerate the HR further. The independent regulation of the sympathetic nervous system (SNS) and the parasympathetic nervous system (PNS) creates a diverse pool of possible shifts in dominance as both sympathetic and parasympathetic activity can increase or decrease at any given time, either to the same extent or in different ratios (see expansion on the topic in the Discussion section (4), subsection 4.5: Parasympathetic—sympathetic balance during sensorimotor integration). The ability to engage in different ANS activity patterns allows for flexible modulation of cardiac activity to meet diverse environmental demands (Weissman and Mendes 2021).

Heart rate variability (HRV), the variation in time intervals between consecutive heartbeats, is an indicator of cardiac vagal tone, which represents the contribution of the parasympathetic nervous system to cardiac regulation (Laborde et al. 2017; Malik et al. 1996). An optimal (high) level of resting HRV indicates healthy function and predicts efficient self-regulatory capacity (McCraty and Shaffer 2015). Conditions where self-regulation is needed (e.g., when the individual is facing a physical or mental stressor) typically result in HR acceleration due to a dominance shift in ANS mode of action from PNS to SNS control, triggered also by a high level of vagal withdrawal (decrease in HRV) (Holzman and Bridgett 2017). The magnitude of the drop in HRV indicates adaptability and the inherent capacity of the individual to switch between safety and threat states (Smith et al. 2020). Consequently, HRV is considered a measure of neurocardiac function that reflects the extent to which the system provides flexible and adaptive regulation of its periphery to provide the needed resources to face upcoming events (McCraty and Shaffer 2015).

1.3 | Virtual Reality-Based Sensorimotor Incongruence Paradigm to Delineate Autonomic Nervous System (ANS)–Sensory–Locomotion Interactions

The entrance of virtual reality (VR) paradigms to the behavioral neuroscience arena enables the delineation of the integrative perception-action behaviors across motor and sensory functional domains (Elor and Kurniawan 2020; Alameda-Pineda et al. 2019). VR environments immerse participants in scenarios that resemble the real world while allowing them to manipulate sensory inputs, consequently inducing physiological responses otherwise not possible. At the same time, our ability to control artificially the content and the sensory inputs in the VR environments allows us to 'tease out' the relative roles of the different functional modalities in perception and action, as we previously demonstrated with the role of vision in gait modulation. In this previous work, which aimed at describing the different contributions of sensorial cues to inclined walking modulations, we formed a fully immersive VR environment that enables dissociation of the impact of visual and physical body-based cues, that is allowing sensorimotor incongruence. We tested conditions in

which the inclination of the visual scene is either congruent or incongruent with the physical inclination of the walking surface. Our results demonstrated that purely visual cues (from virtual-only inclines) induce consistent locomotor adaptations to counter expected gravity-based changes, following the indirect prediction principles that is downhill virtual visual cues activate the braking effect, reflected in a temporal trough in gait speed, and uphill virtual visual cues promote an exertion effect, reflected by a temporal peak in gait speed (Cano Porras et al. 2020; Benady, Zadik, Ben-Gal, et al. 2021; Benady, Zadik, Zeilig, et al. 2021).

In the present work, the interrelations between locomotion control, gravity-related sensory inputs, and ANS function are at the focus. We aim to investigate the sensitivity of the ANS to congruent versus non-congruent visual information, as expressed by HR and HRV measures. Following our previous results, in which we showed that purely visual cues triggered adaptive gait patterns (i.e., braking and exertion effects), we expect to observe alterations in ANS action modes that are driven by visual-only cues. This is an exploratory study; however, we hypothesize that during non-congruent conditions, the PNS-SNS balance will be shifted toward PNS withdrawal.

2 | Materials and Methods

2.1 | Participants

We analyzed ECG data of participants performing the 'Sensorimotor incongruence' paradigm, which was performed using a large-scale VR environment developed in our lab, incorporating a movable platform with an embedded treadmill (TM) (Cano Porras et al. 2020; Benady, Zadik, Ben-Gal, et al. 2021).

Data of young healthy adults ($n = 14$; age 26.07 ± 3.08 (mean ± SD); 6 females) were collected in two similar experimental procedures (Benady, Zadik, Ben-Gal, et al. 2021; Benady, Zadik, Zeilig, et al. 2021) (see Procedure section below and section A, Table S1). Results of gait analysis derived from this data collection are reported elsewhere (Benady, Zadik, Ben-Gal, et al. 2021; Benady, Zadik, Zeilig, et al. 2021). Exclusion criteria were physical and visual restrictions, motor impairments, or cognitive and psychiatric conditions that could potentially affect locomotion or the capability to comply with instructions. An exploratory sample size strategy was adopted due to the absence of prior comparable studies quantifying ANS responses from participants subjected to physical-visual sensory incongruence. In choosing this approach, we prioritized hypothesis generation assuming effect size in the medium range, that is 0.1 in partial Eta square terms ($\eta_p^2 = 0.1$). Sample size estimation was performed using GPower (Faul et al. 2007) employing a within-subject repeated measures model with six different conditions (2 visual manipulations and 3 behavioral periods) and two primary outcomes (i.e., HR and HRV). To account for multiple comparisons by adjusting Alpha (0.05), our calculations suggest that data from a minimum of 12 participants is needed. The experimental protocol was approved by the Sheba Medical Center institutional review board (IRB). All participants signed a written informed consent prior to enrolling in the study.

2.2 | Apparatus

2.2.1 | Virtual Reality System

A fully immersive virtual reality system (CAREN High-End, Motek Medical, The Netherlands) projected the virtual environment stimuli on a full-room dome-shaped screen surrounding the participant. The system is equipped with a movable platform with six degrees of freedom, which enables changing the inclination of the walking surface (e.g., level, uphill, downhill). The platform has an embedded treadmill that operates in a self-paced (SP) mode, allowing participants to walk naturally (Kimel-Naor et al. 2017; Plotnik et al. 2015), in synchronization with the 3D virtual environment (Figure 1A). A tachometer in the TM's motor provided the velocity signals from the TM's belts. Elements of the experimental system are shown in Figure 1A.

2.2.2 | Physiological Measures Recording—Electrocardiogram (ECG)

To assess cardiac dynamics, the electrical activity of the heart was recorded during experimental sessions using an electrocardiogram (ECG). Surface-wired self-adhesive electrodes were attached under the right clavicle and over the heart apex prior to testing, along with a recording amplifier. HR was continuously recorded at 1024 Hz using a portable system (eego sports, ANT Neuro, the Netherlands) that was automatically synchronized with session events for post hoc analysis.

2.3 | Procedure

The experimental procedure is fully described in previously published work (Benady, Zadik, Ben-Gal, et al. 2021; Benady, Zadik, Zeilig, et al. 2021). Herein, it is briefly described.

2.3.1 | Habituation to Self-Paced Treadmill Walking

First, participants were given free time for level walking to become familiar with the system and feel comfortable walking in SP. Afterwards, they completed three training trials in which they performed SP walking in the three visual-motor congruent inclines (e.g., visual and motor both in a level position, uphill or downhill).

2.3.2 | Sensorimotor Incongruence Paradigm

The visual scene of the sensorimotor incongruence paradigm included a park landscape with the participant walking on a 3.6-m-wide path. The visual field progressed at a similar rate to the participant's walking speed. The visual (virtual) incline effect was achieved by projecting the path with an upward incline, that is above the virtual horizon line (uphill; Figure 1B, left column), or with a downward incline, that is under the virtual horizon line (downhill; Figure 1B, right column). When simulating leveled scenery, the path converged with the line of the virtual horizon (leveled; Figure 1B, middle column).

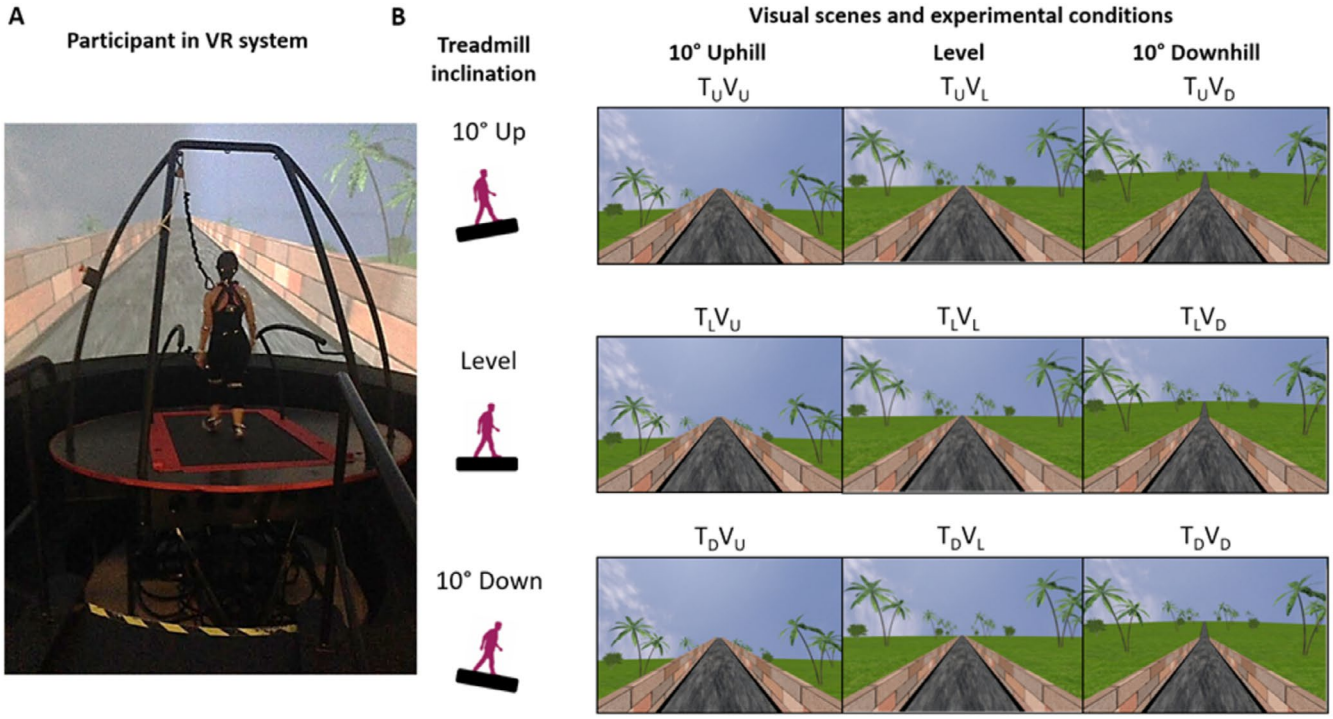

FIGURE 1 | Apparatus and experimental conditions. (A) A fully immersive virtual reality system projected the virtual environment stimuli on a full-room dome-shaped screen surrounding the participant. The system includes a movable platform with six degrees of freedom, which enables changing the inclination of the walking surface (e.g., level, uphill, downhill). (B) The testing protocol included nine randomly presented experimental conditions, in which the inclination of the visual scene was either congruent or incongruent with the physical inclination of the treadmill (TM). In B, rows represent TM inclination, and columns represent visual scene inclination. TM and visual scene congruent conditions appear on the diagonal for uphill (T_UV_U), level (T_LV_L), and downhill (T_DV_D) walking. TM and visual scene incongruent conditions include the following: While the TM was in an uphill incline, the visual scene was leveled (T_UV_L) or downhill (T_UV_D); while the TM was leveled, the visual scene was uphill (T_LV_U) or downhill (T_LV_D); and lastly, while the treadmill was in a downhill incline, the visual scene was leveled (T_DV_L) or uphill (T_DV_U). Adopted from (Cano Porras et al. 2020).

Participants began all trials from a standstill position and started walking with both the TM and the visual scene leveled until reaching steady state velocity (SSV; a consecutive period of 12 s with walking speed coefficient of variance less than 2%). Following that, a transition (of the platform and/or visuals) occurred to one of the experimental conditions as described below. Prior to each of the experimental conditions, participants were given the instructions to walk "as naturally as possible" and that "the incline might change during walking". Post-transition, participants walked for an additional 65 s.

The experimental protocol included nine randomly presented experimental conditions, in which the inclination of the visual scene was either congruent or incongruent with the physical inclination of the TM. The TM (T) and/or visual scene (V) transitioned to +10° uphill (U), remained in a level position at 0° (L), or transitioned to −10° downhill (D). Figure 1B describes the experimental conditions where rows represent the TM incline, and columns represent the visual scene incline. TM and visual scene congruent conditions (baseline conditions) appear on the diagonal for uphill (T_UV_U), level (T_LV_L), and downhill (T_DV_D) walking. TM and visual scene incongruent conditions include the following: while the TM was in an uphill incline, the visual scene was leveled (T_UV_L) or downhill (T_UV_D); while the TM was leveled, the visual scene was uphill (T_LV_U) or downhill (T_LV_D); and lastly, while the treadmill was in a downhill incline, the visual scene was leveled (T_DV_L) or uphill (T_DV_U).

2.4 | Outcome Measures and Analyses

The analysis described in this work was focused on the ANS function reflected in the cardiac reactivity of participants subjected to visual-physical incongruence. The analyses were conducted using MATLAB software (version R2020b, MathWorks Inc., Natick, MA, USA). Specifically, we established the physiological baseline of participants walking in the level congruent condition (i.e., no physical nor visual inclines) and compared it to incongruent conditions in which the treadmill was level, but visuals indicated uphill or downhill. In addition, we expanded the analysis to explore the effect of visual-physical incongruence also for uphill and downhill TM conditions (i.e., inclined walking).

2.4.1 | Heart Rate Related Outcome Measures—Level Walking Conditions

2.4.1.1 | Baseline Relation Between Heart Rate (HR) and Gait Speed—Linear Calibration. To account for HR changes which were driven by changes in walking speed (and not due to the sensorimotor incongruence), we calculated the HR to gait-speed baseline relation (linear calibration; $HR = aV + b$; where V is the gait speed) for each participant through his/her data from level congruent walking conditions. The calibration was based on data points extracted

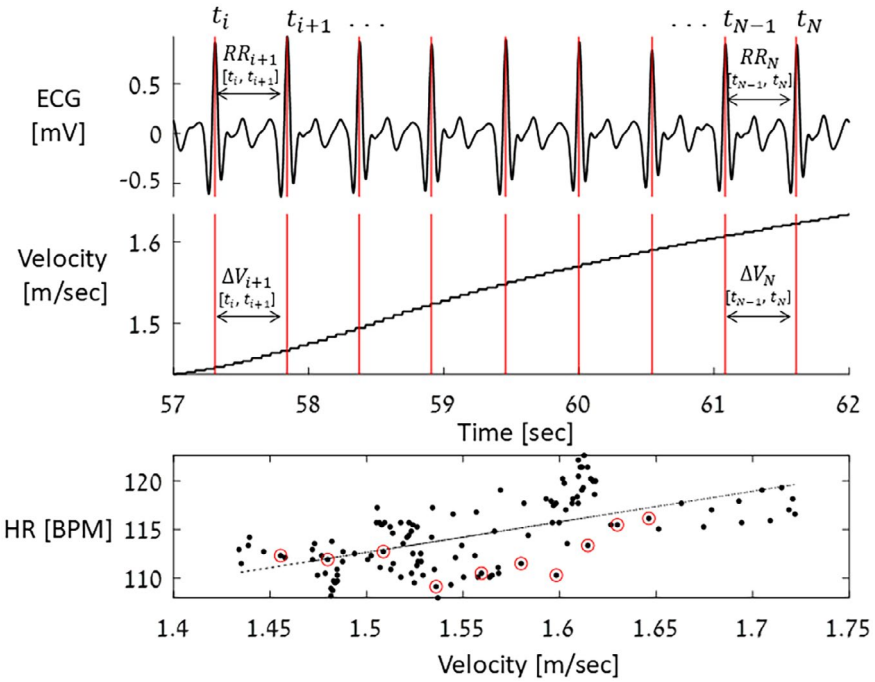

FIGURE 2 | Heart rate to gait-speed baseline relation calculation scheme. A demonstration of the calibration calculation, which was based on ECG data extracted from congruent level walking periods, for each participant (top panel; 5 s sample from one participant). During these periods, we assigned time stamps to each heartbeat (t_i; red bars) and calculated the time differences between consecutive heartbeats (i.e., RR interval; top panel) from which we further calculated the instantaneous HR values. Each instantaneous HR value was paired with a gait speed value, which is the mean gait speed during the same time interval $[t_i, t_{i+1}]$ (middle panel). We used the linear fit function ($HR = aV + b$; where V denotes gait speed) to determine, for each participant, the relation between HR and gait speed (bottom panel; in this example, the Pearson's coefficient is $r = 0.61$, $p < 0.001$). Circled data points (bottom panel) correspond to the heartbeats and average velocity values marked in red bars (top and middle panels, respectively). BMP-beats per min.

from all congruent level walking periods, per participant that is one full session of level walking ($T_L V_L$; Figure 1B, middle panel) and eight more time-segments spanning from the start of the test until start of transition (all other experimental conditions; Figure 1B, all surrounding panels), which were also times of congruent level walking. During these periods, we assigned time stamps to each heartbeat (according to the R peaks locations in the ECG, t_i; i- running index) and extracted the time differences between consecutive heartbeats (i.e., RR intervals; $RR_{i+1} = t_{i+1} - t_i$). To avoid false detections due to noise, we then pre-processed the RR vectors by handling outliers. We used the 'mean' method to detect the outliers (i.e., detecting elements more than 3 standard deviations above the mean) and replaced them with the average of neighboring RR's, resulting in an NN intervals vector (normal to normal intervals). Instantaneous HR values (beats per min; BPM) from the pool of congruent level data points, for each participant, were then calculated based on the formula:

$$\text{instantaneous HR}\left(t_{i+1}\right)[\text{BPM}] = {}^{60}/_{(NN_{i+1})} \quad (1)$$

where the value of the instantaneous HR was assigned to the occurrence of the second heartbeat (at time t_{i+1}). Each instantaneous HR value was paired with a gait speed value (V), which is the mean gait speed in the same time interval $[t_i, t_{i+1}]$. With these two vectors of values, instantaneous HR and V, we turned to define the linear relation. We used the linear fit function ($HR = aV + b$) to determine, for each participant, the relation between HR and gait speed. The entire process is illustrated in Figure 2. All linear calibrations were statistically significant ($p < 0.001$), and Pearson's r indicated a positive linear relation for all participants (i.e., higher HR for higher velocity).

2.4.1.2 | Real-to-Expected Heart Rate Delta. Once we established the individual baseline relation between HR and gait speed in the level congruent condition for each participant, we calculated the variation between the recorded HR from the incongruent conditions to that expected according to the linear calibration curve. We calculated the relative difference (percentile) between measured HR (i.e., real HR) and the values estimated by the calibration curve (i.e., expected HR) as follows:

$$\text{HR Diff}\,[\,\%\,] = 100 \times \left({}^{\text{HR observed} - \text{HR expected}}/_{\text{HR expected}}\right) \quad (2)$$

This metric, which contains the residual alteration of HR driven by the sensorimotor incongruence, is referred to here as the relative real-expected HR delta (see Figure 3A).

2.4.1.3 | Heart Rate Variability. To characterize HR reactivity and sensitivity to sensorimotor incongruence, we used the time differences between consecutive heartbeats (i.e., RR intervals) to calculate heart rate variability (HRV) measures in the time and frequency domains. We calculated the root mean square of successive NN interval differences (RMSSD)

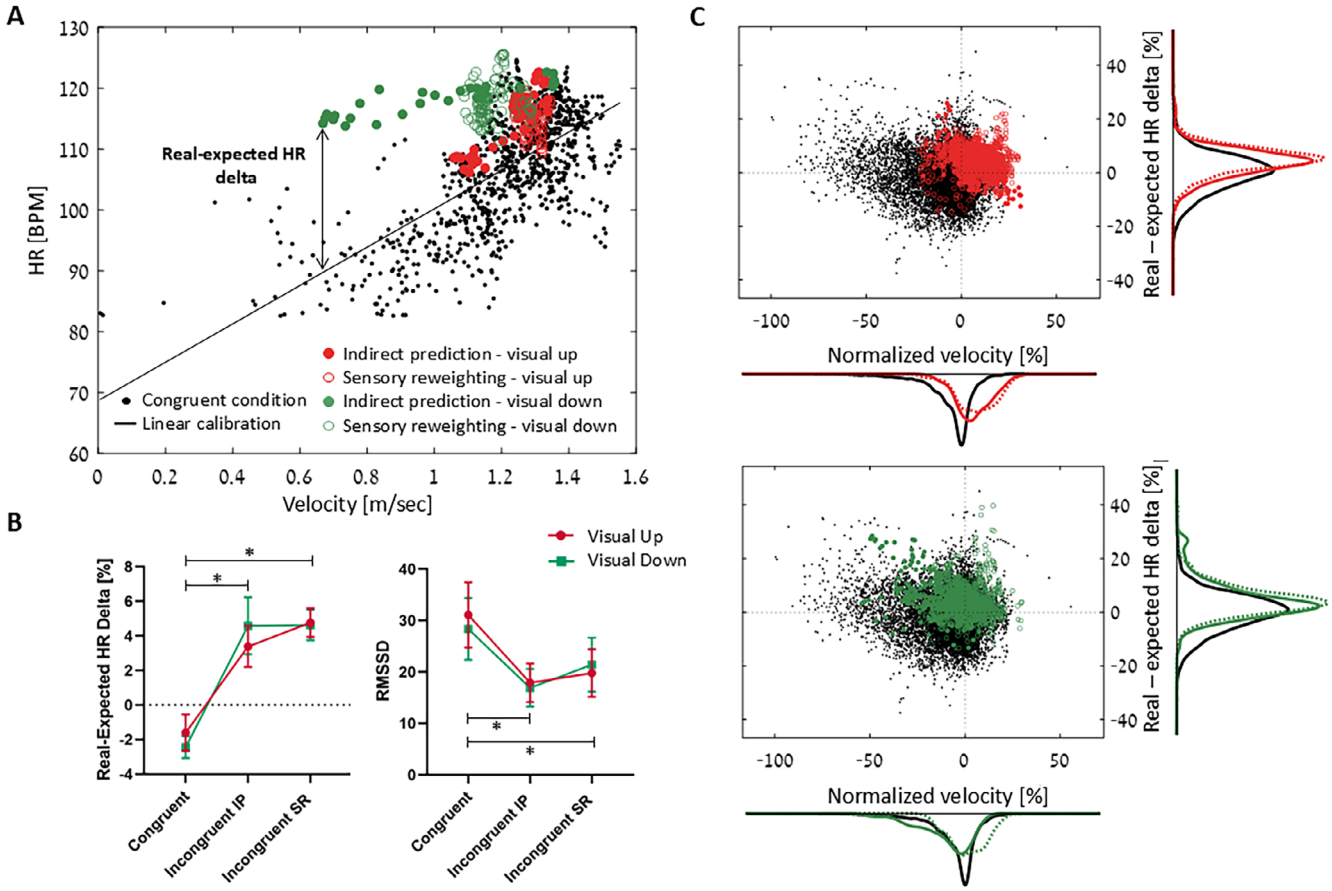

FIGURE 3 | Altered cardiac function during incongruent periods of level walking. (A) Calculation of the HR to gait-speed linear calibration for each participant using his/her data from congruent walking conditions (black dots; data of one participant). Differences between measured HR extracted from the incongruent periods (colored circles) and the expected HR (fitted line) are calculated as real-expected HR delta (in %). Average values of the real-expected HR delta and the RMSSD across participants ($n = 14$) are presented in (B). Asterisks indicate a statistically significant difference between a pair of means ($p < 0.001$), error bars represent standard errors. (C) Grouped marginal distributions of the real-expected HR delta against the normalized walking speed, across participants ($n = 14$). Black dots represent the congruent data set extracted from all participants (in histograms-black line). Colored dots represent the incongruent periods of visual uphill (upper panel; red dots and lines) and downhill (bottom panel; green dots and lines). Solid versus dotted lines represent the IP and SR periods, respectively. This figure demonstrates that visual-physical incongruence is associated with altered cardiac function. Similar analyses for downhill and uphill walking are presented in Figures 4 and 5, respectively. IP, indirect prediction; SR, sensory reweighting.

and the High frequency (HF) power bands (see Supporting Information, Section B, for methodological description of calculation) both reflecting parasympathetic activity, and the standard deviation of consecutive NN intervals (SDNN) which assesses both sympathetic and parasympathetic contributions (Laborde et al. 2017; Malik et al. 1996; Shaffer and Ginsberg 2017). The RMSSD outcome measure was chosen here as a representative metric for HRV due to the following reasons: (i) RMSSD is directly related to the parasympathetic system, reflecting vagal tone; (ii) Although being highly correlated to the high frequency power band, reflecting also the vagal tone, the RMSSD is relatively free of respiratory influences (Laborde et al. 2017; McCraty and Shaffer 2015; Kleiger et al. 2005; Dionne et al. 2002; Larsen et al. 2010); and (iii) RMSSD provides meaningful information also in short and ultra-short time intervals (i.e., 10–50 s) (Laborde et al. 2017; Salahuddin et al. 2007; Munoz et al. 2015). The average length of recordings (across participants, per condition) is described in the Section C–Table S2. In general, samples were longer than 10 s. In the body of the article, we report on RMSSD. SDNN and HF results are brought in the Supporting Information, sections B, G–I; see the results (3) for more details.

2.4.1.4 | Segmentation of Walking Sessions Into Behavioral Periods. We implemented Laborde et al. (2017) approach to HRV analysis, which advises that cardiac data sets should be divided into—and compared between—three behavioral domains, namely, resting (i.e., baseline), reactivity (i.e., immediate response to an event) and recovery. Accordingly, we segmented all level walking sessions as follows: (i) congruent period that is baseline; defined as the time between the beginning of the experiment, through the 12 s of SSV until transition that is the change in the visual scenery to inclined path. The consecutive 65 s timeframe after transition was also segmented into (ii) indirect prediction (IP) period that is reactivity to the change in the visual flow; time period between transition until twice the duration of reaching the maximal change in walking speed from steady state (either peak or trough) and (iii) sensory reweighting (SR) period that

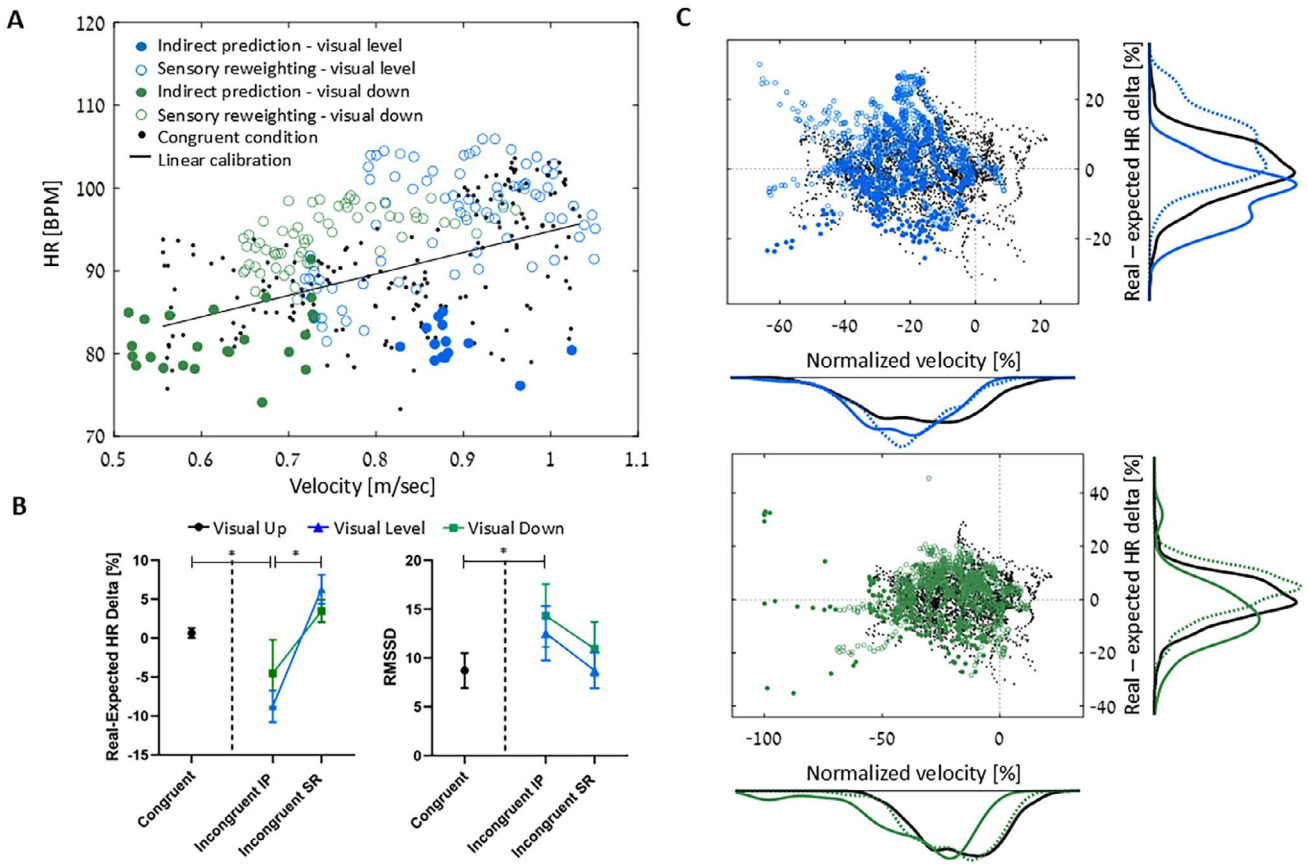

FIGURE 4 | Altered cardiac function during incongruent periods of uphill walking. (A) Calculation of the HR to gait-speed linear calibration for each participant using his/her data from uphill congruent walking conditions (black dots; data of one participant). Differences between measured HR extracted from the incongruent periods (colored circles) and the expected HR (fitted line) are calculated as real-expected HR delta (in %). Average values of the real-expected HR delta and the RMSSD across participants ($n = 10$) are presented in (B). Asterisks indicate a statistically significant difference between a pair of means ($p < 0.05$), error bars represent standard errors. (C) Grouped marginal distributions of the real-expected HR delta against the normalized walking speed across participants ($n = 10$). Black dots represent the uphill congruent data set extracted from all participants (in histograms- black line). Colored dots represent the incongruent periods of visual level (upper panel; blue dots and lines) and visual downhill (bottom panel; green dots and lines). Solid versus dotted lines represent the IP and SR periods, respectively. This figure demonstrates that visual-physical incongruence is associated with altered cardiac function. IP, indirect prediction; SR, sensory reweighting.

is recovery; between the end of the IP period and the end of the session. From the initial congruent segment, we discarded the first 10% as the walking speed was only slightly above zero. A gallery of individual calibration data and fitted lines with detailed significance and coefficients, including the individual incongruent data points divided into IP and SR periods, is presented in the section D–Figure S2.

2.4.2 | Heart Rate Related Outcome Measures—Uphill and Downhill Walking Conditions

As detailed above, the experimental paradigm was such that the participant always started walking in a TM-level vision level condition. Thus, in the analysis of level walking conditions, we could compare three sequential behavioral periods (i.e., congruent, incongruent IP, and incongruent SR). This could not be done for the TM up or TM down conditions. Therefore, the outcome measures and analyses for the uphill and downhill walking conditions were calculated differently as described below.

Congruent data available in the uphill and downhill walking conditions could be derived only from the one appropriate congruent condition (i.e., T_UV_U and T_DV_D, respectively; 60s timeframe after platform transition, which lasts 5s, ends). To strengthen the individual HR to gait-speed calibrations by increasing the congruent data set, we included the corresponding inclined training trials data (i.e., uphill and downhill) in the pool of congruent data used for the calibration. We then calculated the HR to gait-speed baseline relation (linear calibration) for each participant as described above for level walking (see section 2.4.1.1). All linear calibrations were calculated for the congruent uphill and downhill conditions, but two were statistically significant ($p < 0.05$). Then, in a similar manner to the level walking analysis (see sections 2.4.1.2 & 2.4.1.3), the real-expected HR delta and HRV parameters (RMSSD and SDNN) were calculated.

Data from the congruent uphill and downhill walking conditions served as a non-chronological baseline to which we compared the IP and SR periods, which were segmented similarly to the practice used in the level walking analysis. Briefly,

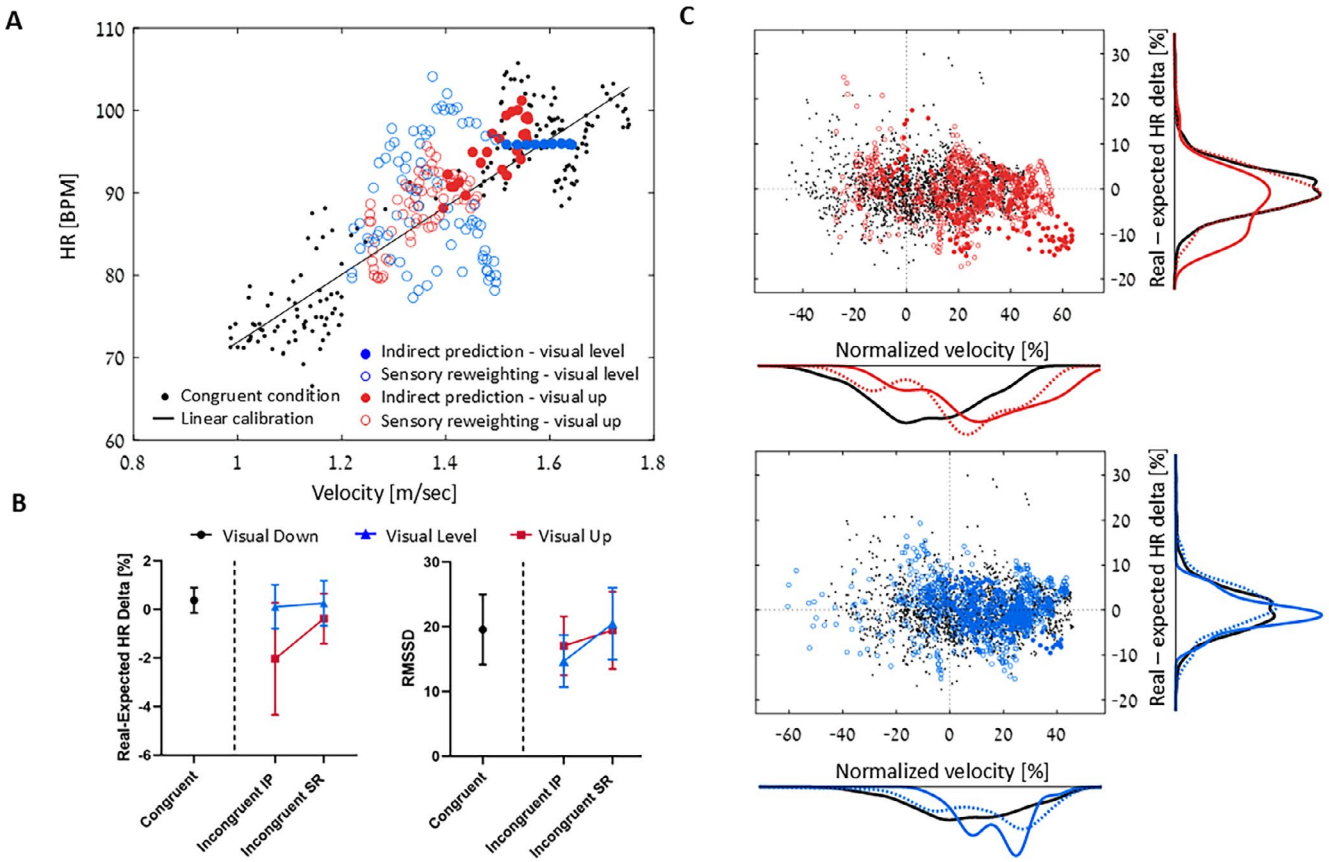

FIGURE 5 | No effect of incongruent periods on cardiac function in downhill walking. (A) Calculation of the HR to gait-speed linear calibration for each participant using his/her data from downhill congruent walking conditions (black dots; data of one participant). Differences between measured HR extracted from the incongruent periods (colored circles) and the expected HR (fitted line) are calculated as real-expected HR delta (in %). Average values of the real-expected HR delta and the RMSSD across participants are presented in (B). Error bars represent standard errors. (C) Grouped marginal distributions of real-expected HR delta against the normalized walking speed, across participants ($n = 10$). Black dots represent the downhill congruent data set extracted from all participants (in histograms- black line). Colored dots represent the incongruent periods of visual uphill (upper panel; red dots and lines) and visual level (bottom panel; blue dots and lines). Solid versus dotted lines represent the IP and SR periods, respectively. IP, indirect prediction; SR, sensory reweighting.

segmentations of uphill and downhill walking sessions were carried out as follows: (i) congruent period that is baseline; derived from the relevant congruent conditions (i.e., T_UV_U and T_DV_D, respectively; 60 s timeframe after platform transition has ended) (ii) indirect prediction (IP) period that is reactivity to the change in walking conditions; time period between the end of transition until twice the duration of reaching the maximal change in walking speed from SSV (either peak or trough) and (iii) sensory reweighting (SR) period that is recovery; between the end of the IP period and the end of the session. A gallery of individual calibration data and fitted lines with detailed significance and coefficients, including the individual incongruent data points divided into IP and SR, are presented in the sections E and F–Figures S3 and S4 for uphill and downhill, respectively.

2.4.3 | Walking Speed Related Outcome Measures

Gait analysis was not the focus of this study, yet we also aimed to demonstrate the association between the ANS and motor responses to visual–physical incongruence. To that end, we calculated walking speed-related variables in a manner similar to that published in our previous work (Benady, Zadik, Ben-Gal, et al. 2021; Benady, Zadik, Zeilig, et al. 2021), where detailed descriptions are provided. Briefly, to establish the post-transition effects on gait speed, we assessed the following: (i) the magnitude of the peak/trough of gait speed relative to the SSV (presented in %) and (ii) the time of this peak from the start of transition (seconds).

Additionally, conforming to our previous definitions (Benady, Zadik, Ben-Gal, et al. 2021; Benady, Zadik, Zeilig, et al. 2021), walking speed (WS) outcomes reported here are normalized by the individual SSV as follows: we divided the WS in each condition by the average SSV of the specific session. Subsequently, we subtracted the average SSV value from the resulting trace to set the normalized WS to approximately zero at the time of transition. Therefore, normalized WS represents the percent change in WS relative to SSV. Ultimately, in a post hoc analysis we confirmed that there was no 'order effect' on values of baseline walking speed: a Repeated measure analysis of variance (RM-ANOVA) in a within-subjects factor design revealed no main effect of Order (condition's appearance order, 9 levels) on the average SSV ($F_8 = 1.26$, $p = 0.31$).

2.5 | Statistical Analyses

Statistical analyses for this study were run using JASP software (JASP Team (2023), version 0.17.3). The statistical significance level was set at $p < 0.05$.

2.5.1 | Level Walking Conditions

The real-expected HR delta and RMSSD outcome measures were calculated per subject ($n = 14$), per consecutive behavioral periods ($n = 3$; congruent, incongruent-IP, incongruent-SR), and per type of visual incongruence ($n = 2$; T_LV_U and T_LV_D). RMSSD yields one value to assess per period, and the final value of the real-expected HR delta is the average of all HR deltas in a period. Our primary hypothesis (see introduction) predicts PNS withdrawal during incongruent periods, characterized by increased HR and decreased HRV compared to congruent periods. RM-ANOVA was used to assess the main effects of behavioral period (congruent, incongruent-IP, incongruent-SR; within-subjects factor), type of visual incongruence (vision up, vision down; within-subjects factor), and Behavioral period × Visual incongruence interaction on the real-expected HR delta and RMSSD. Partial Eta Squared (η_P^2) was computed as a measure of effect size. In pre-hoc analyses, Shapiro–Wilk normality tests were conducted in each behavioral period ($n = 3$) and Visual incongruence ($n = 2$) groups. Normality tests indicated a normal distribution of the real-expected HR delta and a non-normal distribution for the RMSSD measure. Accordingly, RMSSD data were log-transformed prior to employing the ANOVA test. We then confirmed that all outcome measures sphericity (i.e., equal variances of the differences between all groups) using Mauchly's test ($p > 0.05$). The Bonferroni correction was used to adjust the post hoc p-values of the ANOVA.

2.5.2 | Uphill and Downhill Walking Conditions

As a first step, we conducted a two-way RM ANOVA on the sequential IP and SR periods (without the congruent period, which was extracted from a different trial—see section 2.4.2). We assessed the main effects of behavioral period (incongruent-IP, incongruent-SR; within-subjects factor), type of visual incongruence (vision level, vision up or vision down; within-subjects factor), and Behavioral period × Visual incongruence interaction, on the real-expected HR delta and the RMSSD. From this step, we established there was no visual incongruence effect ($p > 0.064$) nor an interaction between the factors ($p > 0.14$) in both outcome measures, in both uphill and downhill. Therefore, we continued to conduct a one-way RM ANOVA to compare each group of different walking conditions, now also including the congruent walking condition, testing for a main effect of Walking condition. In this analysis step, we had a total of 5 groups per TM incline ($n = 2$) we compared for both outcome measures. In pre-hoc analyses, Shapiro–Wilk normality tests were conducted in each Walking condition ($n = 5$) and TM incline ($n = 2$) groups. Normality tests indicated normal distributions of the real-expected HR delta and partial non-normal distributions in the RMSSD measure (5/10 were normally distributed). Accordingly, the RMSSD data were log-transformed prior to employing the ANOVA tests. The Bonferroni correction was used to adjust the post hoc p-values of the ANOVA.

2.5.3 | Correlation Analysis

Linear relations were assessed and fitted using Pearson's correlation analyses conducted on log-transformed RMSSD data sets (to comply with the normality assumption).

3 | Results

3.1 | Level Walking Conditions

In these conditions (Figure 1B; middle row), we analyzed data from 14 participants who completed TM level walking segments while the visual field was translated to uphill scenery (T_LV_U; color coded in red in Figure 3) and 14 segments where it was translated to downhill scenery (T_LV_D; color coded in green in Figure 3). Each of these walking segments provided HR data from three behavioral periods (i.e., Congruent, incongruent-IP, incongruent-SR; recall statistical analyses in the Methods section). In this section, we tested whether the incongruent visual stimuli, that is visual uphill and visual downhill, influence HR and HRV. Statistical analysis revealed a main effect of behavioral period on the real-expected HR delta measure ($F_{2,26} = 35.71$, $p < 0.001$, $\eta_P^2 = 0.73$; higher values in incongruent periods). Post hoc analysis revealed that the source of the difference was in the pairwise comparisons of the Congruent period to both the incongruent-IP and incongruent-SR periods ($p < 0.001$ in both comparisons; Figure 3B, left panel). Similarly, statistical analysis revealed a main effect of behavioral period ($F_{2,26} = 25.21$, $p < 0.001$, $\eta_P^2 = 0.66$; lower values in incongruent periods) on the RMSSD measure. The source of the effect is, again, the differences between the Congruent period and both the incongruent-IP and incongruent-SR periods ($p < 0.001$ in both comparisons; Figure 3B, right panel). No effect of Visual incongruence was found on the HR delta ($F_{1,13} = 0.003$, $p = 0.95$, $\eta_P^2 < 0.01$) nor on the RMSSD ($F_{1,13} = 0.67$, $p = 0.43$, $\eta_P^2 = 0.05$) outcome measures. None of the Behavioral period × Visual incongruence interactions were found significant ($F_{2,26} = 1.06$, $p = 0.36$, $\eta_P^2 = 0.08$ and $F_{2,26} = 1.11$, $p = 0.34$, $\eta_P^2 = 0.08$ for the real-expected HR delta and RMSSD outcome measures, respectively). SDNN results are detailed in the section G – Figure S5. These effects demonstrate that HR and HRV were indeed affected by the incoherent visual information, regardless of the specific visual manipulation (i.e., up/downhill).

Specifically, HR deltas during the incongruent periods were considerably higher in comparison to the congruent level walking period, both in vision up and down conditions, as demonstrated by the real-expected HR delta measure (Figure 3B, left panel). While in the congruent periods HR delta demonstrates a small negative deviation from the calibration for example $-1.60\% \pm 1.06\%$ (mean ± SE) and $-2.44\% \pm 0.64\%$ for vision up and down, respectively, in the incongruent periods we found all positive HR deltas as follows: vision up: 3.39 ± 1.19 and 4.76 ± 0.83 for the incongruent-IP and incongruent-SR, respectively; vision down: 4.58 ± 1.65 and 4.62 ± 0.88 for the incongruent-IP and

incongruent-SR, respectively. While the HR was increasing in the incongruent periods post-transition, RMSSD responded with a considerable decrease (withdrawal) in the IP period, which also lasted through the later SR period (Figure 3B, right panel). Specifically, RMSSD values were 31.09 ± 6.34, 17.91 ± 3.74, and 19.78 ± 4.64 for the congruent, incongruent-IP, and incongruent-SR of the visual up condition, respectively. A similar trend was captured in the visual down condition.

Figure 3C demonstrates the distributions of all real-expected HR delta (pooled data from all participants) against normalized walking velocity (pooled data from all participants, normalized by individual SSV) extracted from the congruent data pool (i.e., data used for the calibration; black dots) and from the incongruent periods (IP and SR; colored circles, see key in panel A). As TM stayed leveled and vision transitioned to uphill (Figure 3C, upper panel), participants demonstrated an increase in walking velocity compared to congruent conditions (e.g., exertion effect (Cano Porras et al. 2020; Benady, Zadik, Ben-Gal, et al. 2021)). This behavioral change was associated with positive HR deltas, depicted in the positioning of most of the incongruent data set (red circles) above the zero line (upwards shift). This is also apparent for the vision down condition (Figure 3C, bottom panel) where gait speed values, which are slightly shifted to the left (lower velocities due to the braking effect (Cano Porras et al. 2020; Benady, Zadik, Ben-Gal, et al. 2021)) are associated with positive HR deltas.

3.2 | Uphill Walking Conditions

We also analyzed data from 10 participants who completed walking segments during which the TM transitioned to an uphill incline while the visual field stayed in level scenery (T_UV_L; color coded in blue in Figure 4), and 10 segments where the visual field was translated to downhill scenery (T_UV_D; color coded in green in Figure 4). Each of these walking segments provided HR data from two periods (i.e., incongruent-IP, incongruent-SR), which were also compared to the appropriate congruent condition (T_UV_U). Statistical analysis revealed a main effect of Walking condition on the real-expected HR delta measure ($F_{4,36} = 7.92$, $p < 0.001$, $\eta_P^2 = 0.47$; groups are different). Post hoc analysis revealed that the source of the difference was in the pairwise comparisons of the congruent period to the incongruent-IP and between the incongruent-IP and the incongruent-SR periods of vision level ($p < 0.05$ in both comparisons; Figure 4B, left panel). Similarly, for the RMSSD measure, statistical analysis revealed a main effect of walking condition ($F_{4,36} = 3.80$, $p = 0.04$, $\eta_P^2 = 0.30$; groups are different), the source of which is in the comparison of the congruent to the incongruent-IP periods in vision down ($p < 0.05$; Figure 4B, left panel). SDNN results are detailed in the section H – Figure S6. These effects demonstrate yet again that HR and HRV were affected by the incoherent visual information.

Specifically, HR of participants during the incongruent-IP periods was lower (negative deltas) in comparison to the expected (which is based on congruent data), followed by a substantial recovery in the incongruent-SR periods, slightly surpassing the Congruent period level, both in vision level and down conditions (Figure 4B, left panel). For the Congruent period, the real-expected HR delta measure was close to zero (0.68 ± 0.62), values extracted from the incongruent-IP are −8.77% ± 2.03% and −4.52% ± 4.33% for vision level and down, respectively. In the incongruent-SR period, the averages reached positive peaks of 6.30% ± 1.86% and 3.49% ± 1.44% for vision level and down.

In the unfolding of the sensorimotor incongruence (i.e., the IP period), as HR values were low relative to the expected due to the visual conflict, RMSSD values were higher than expected and, more importantly, required to face the actual upcoming event, that is an uphill incline. During the late incongruent-SR period, RMSSD values decreased roughly to baseline (Figure 4B, right panel). That is, RMSSD values were 8.72% ± 1.79% at baseline, peaked at 12.54% ± 2.76% in the after event, and were lowered back to 8.73% ± 1.83% in the congruent, incongruent-IP, and incongruent-SR of the visual level condition, respectively. A Similar trend was captured in the visual down condition.

While the distributions of walking velocities (*x*-axis) were not considerably changed between the congruent (Figure 4C; black dots) and the incongruent periods (Figure 4C; colored circles) in the uphill walking conditions, the real-expected HR delta (*y*-axis) demonstrates separation into 3 walking condition-driven distributions: a middle distribution for the congruent condition, which by definition revolves around zero; a negative centered (down shifted) distribution in the IP period (solid line); and a positive centered (up shifted) distribution in the late SR period (dashed line). This tendency was visible both for the level (Figure 4C; upper panel) and down (Figure 4C; lower panel) sensorimotor incongruencies.

3.3 | Downhill Walking Conditions

We analyzed data from 10 participants who completed walking segments during which the TM transitioned to a downhill incline while the visual field stayed in level scenery (T_DV_L; color coded in blue in Figure 5), and 9 segments where the visual field was translated to uphill scenery (T_DV_U; data of one participant were excluded from the analysis due to poor ECG signal quality; color coded in red in Figure 5). Each of these walking segments provided HR data from two periods (i.e., incongruent-IP, incongruent-SR), which were also compared to the appropriate congruent condition (T_DV_D). Statistical analysis revealed no main effect of Walking condition on the HR delta measure nor RMSSD ($F_{4,36} = 0.88$, $p = 0.44$, $\eta_P^2 = 0.09$ and $F_{4,36} = 1.06$, $p = 0.34$, $\eta_P^2 = 0.12$, respectively, groups were not found to be significantly different; Figure 5). SDNN results are detailed in section I – Figure S7.

3.4 | Parasympathetic Reaction to Sensorimotor Incongruence

Log of RMSSD values computed from the whole post-transition period (across IP and SR) from the two types of visual incongruencies, per participant, were found to be linearly correlated. These associations were fitted by means of Pearson's correlation analysis revealing significant positive relations as follows, for level walking ($n = 14$): $r_p = 0.97$, $p < 0.001$; for downhill walking ($n = 9$): $r_p = 0.98$, $p = 0.001$; for uphill walking ($n = 10$): $r_p = 0.97$, $p < 0.001$ (Figure 6). The association of

the participant's individual RMSSD response to incongruent events of different types suggests that the PNS response is robust, activated by the sensorimotor conflict itself rather than by the type of visual manipulation.

3.5 | Parasympathetic—Sympathetic Balance During Sensorimotor Integration

In addition, we explored alterations in parasympathetic and sympathetic balance during sensorimotor incongruence. To that end, we adopted the two-dimensional conception of autonomic space suggested by Berntson et al. (1991) with the parasympathetic ordinate estimated by the normalized RMSSD (across participants i.e., *Z* scores), and the sympathetic abscissa estimated by the normalized SDNN (recall that SDNN is the product of both parasympathetic and sympathetic contributions (Shaffer and Ginsberg 2017)). In Figure 7, data points illustrate group means and standard errors of normalized RMSSD and SDNN values as a function of TM incline; additional information is provided in the Discussion section (4) and the caption of Figure 7.

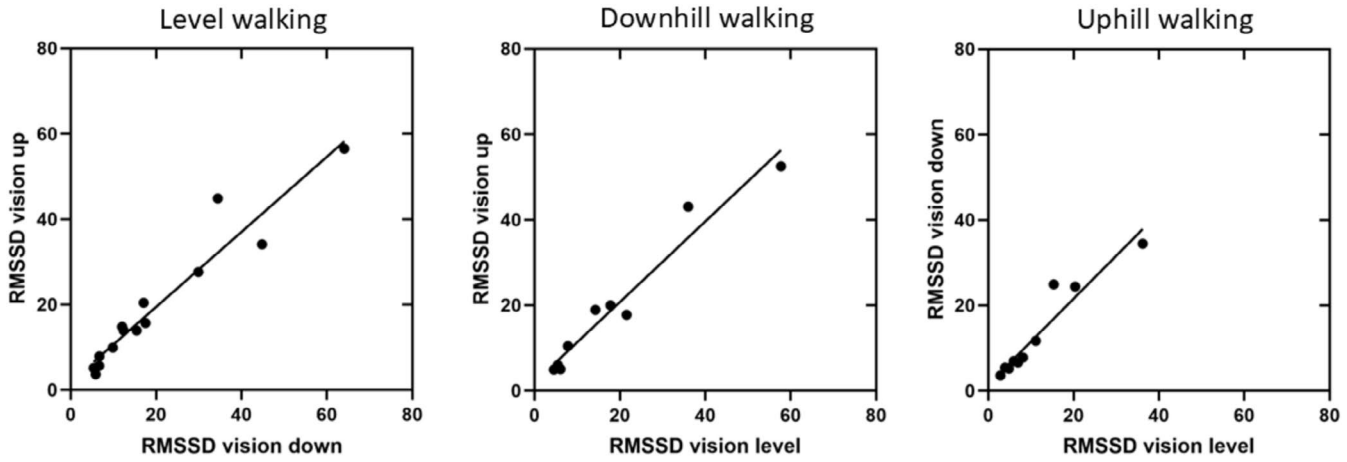

FIGURE 6 | RMSSD response to different types of visual manipulations is correlated. RMSSD values computed from the whole post-transition period (across IP and SR) from the two types of visuomotor incongruencies, per participant, were found to be linearly correlated. The correlations are presented for each TM incline separately. These associations were fitted using Pearson's correlation analysis as follows, for level walking ($n = 14$): $r_p = 0.97$, $p < 0.001$; for downhill walking ($n = 9$): $r_p = 0.98$, $p = 0.001$; for uphill walking ($n = 10$): $r_p = 0.97$, $p < 0.001$.

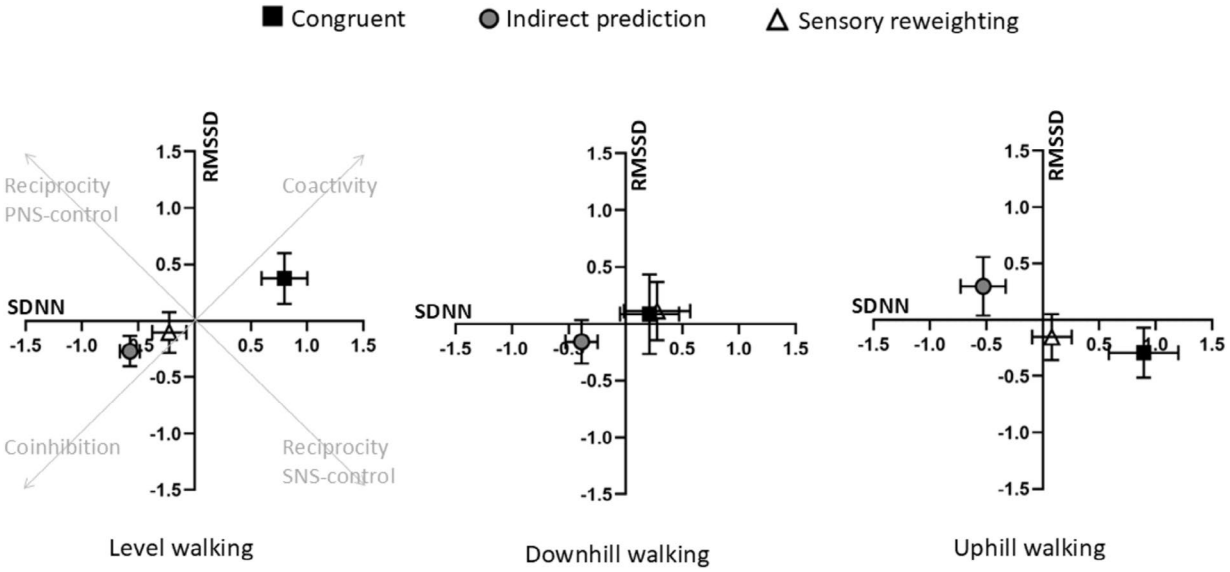

FIGURE 7 | Alterations in the parasympathetic-sympathetic balance during sensorimotor incongruence. To investigate which aspects of parasympathetic/sympathetic balance were altered, we organized RMSSD and SDNN results in the two-dimensional autonomic space defined by Berntson et al. (1991) for each TM incline separately (i.e., level, uphill, and downhill), depicting the positioning of the different behavioral periods investigated in this study (i.e., congruent, incongruent IP, and incongruent SR). The independently regulated sympathetic and parasympathetic stimuli create four joint ANS action modes in which they are either negatively correlated, that is spanning from (a) reciprocity-sympathetic control to (b) reciprocity-parasympathetic control, or positively correlated, that is ranging from (c) coactivation to (d) co-inhibition (left panel in gray). Data points illustrate group means and standard errors of normalized (across participants, i.e., *Z* score) RMSSD and SDNN values as a function of the period, plotted separately for level walking (left panel), downhill walking (middle panel), and uphill walking (left panel).

4 | Discussion

In this study, we explore the involvement of ANS function in gravity-related locomotion regulation during actual and perceived inclined walking. This is the first time, to the best of our knowledge, that self-regulation of gait, that is the IP and SR mechanisms, is shown to be associated with ANS function, as expressed by modulations in the parasympathetic nervous system (PNS) and the sympathetic nervous system (SNS) balance. Using incoherent sensorial cueing, we provided evidence of the responsiveness of HRV to visual information and sensorimotor incongruence during locomotor adaptations (e.g., braking/exertion effects). Taking together with the fact that an ultimate change in gait patterns requires alterations in cardiac resources, we speculate that ANS function and its responsive modes of action are, in fact, facilitating adaptive behavior.

It has already been established that when facing a stressor, a physiological reaction allows temporary adaptation (Ottaviani 2018). The concept of allostasis (the capacity to achieve stability through change (McEwen 1998)) explains the efficient recruitment of body systems (e.g., metabolic, motor etc.) including the ANS in the presence of stress, to re-attain stability through the flexible regulation of internal resources (Thayer and Sternberg 2006; Rodrigues et al. 2020). HRV metrics, which reflect autonomic (im) balance and responsiveness, have been widely utilized as markers of such processes. For example, as repeated activations of the aforementioned responses can be unfavorable to health (Rodrigues et al. 2020), HRV was studied as an indicator of cardiovascular fitness, disease prediction and progress, and mortality (Thayer et al. 2010; Acharya et al. 2006; Soares-Miranda et al. 2014). Associations were also documented between HRV and cognitive performance (Acharya et al. 2006; Forte et al. 2022; Arakaki et al. 2023). In this context, Thayer et al. (2009) and Smith et al. (2017) provided indications of the neural pathways of cardiovascular regulation linking functional units within the CNS that support both goal-directed (top-down) behavior and adaptability (bottom-up) to HRV (Benarroch 1993).

In this work, we provide solid behavioral and physiological evidence in support of a similar mechanism linking changes in the perception of gravity (i.e., by the IMG; in the CNS) to alterations in HR and HRV during locomotion regulation in sensory incongruent circumstances. In the following paragraphs, we will 'dissect' our findings in light of the aforementioned concepts.

4.1 | Level Walking Conditions–The Effect of Incongruence

Incongruent-IP periods in which the TM stayed leveled but the visual scene indicated uphill/downhill inclines triggered the PNS response, reflected in HRV withdrawal (i.e., decreased RMSSD), and a residual increase of HR as compared to congruent conditions (Figure 3). It is plausible that the co-occurrence of cardiac alterations and changes to gait behavior, which were triggered by the incongruent sensorial cues, exhibits the involvement of the ANS in a top-down cascade. It remains, however, to understand why this visually induced alteration in ANS function was not fully recovered by the end of the SR period (65 s from transition). We posit that the long effect period, which surpasses the time the behavioral change is known to be attenuated in (~15 s from transition (Cano Porras et al. 2020; Benady, Zadik, Ben-Gal, et al. 2021)) is the consequence of a prolonged sensory reweighing process, possibly due to the uncertainty associated with the visual conflict and the efforts to resolve it.

4.2 | Uphill Walking Conditions–The Effect of Incongruence

Results from uphill walking conditions support the same notion, although in a slightly different manner. First, all uphill walking RMSSD values are relatively low due to the physical stress uphill walking entails (regardless of the visual incline, in comparison to the required effort in level walking). Nonetheless, in uphill walking, we demonstrated an alteration of HRV and HR that was driven by the incongruent conditions. Values extracted from incongruent IP periods are notably higher than in the congruent condition, reducing to a comparable level of baseline only in the later SR period (Figure 4B). These results suggest that the visual manipulation (in which downhill or leveled surfaces are visually presented while the TM is inclined uphill) caused a temporal delay in the PNS withdrawal that was not yet fully attenuated during the IP period in comparison to the congruent state. As opposed to the fast visually induced activation of sensorimotor integration, efficiently motivating HRV withdrawal in uphill congruent conditions, the conflicted visual cues implied different upcoming events (and metabolic needs), prolonging the sensorial integration and consequently the time to reach the correct precept. The relatively high RMSSD level in the IP period is coupled with lower HR values (i.e., compared to congruent conditions), reinforcing the notion of a delayed mechanism, consequently not facilitating the necessary adaptive allocation of resources for the actual uphill (Figure 4B).

4.3 | Downhill Walking Conditions–The Effect of Incongruence

Downhill walking conditions do not require high levels of exertion due to the gravitational propulsion acting in the direction of walking (contrary to uphill walking). However, the event of the platform transitioning from level to a downhill incline triggers high levels of mental stress, which is related to the momentary instability, perhaps related to the actual physical perturbation and to the fear of uncontrolled acceleration and even falling. Along those lines, we propose that the comparable levels of RMSSD and HR in the incongruent periods of downhill walking (i.e., as compared to congruent conditions; Figure 5) are the consequence of (i) higher stress-driven PNS response, lowering RMSSD levels to baseline faster during the IP period, and (ii) smaller HRV decrease needed to account for the lower level-downhill exertion difference (i.e., as compared to the level-uphill exertion difference).

Notably, real-expected HR delta values from the incongruent IP period in this incline were also the highest in variability, possibly accounting for the individual differences in reaction to the foreseen instability.

4.4 | Parasympathetic Reaction to Sensorimotor Incongruence

We also found that RMSSD levels extracted from paired types of visual manipulation per TM incline were highly correlated. This finding supports that the PNS reaction is individually robust, triggered in a typical manner by conflicting information, regardless of the specific type of visual manipulation. However, we deem that the global shifts in SNS-PNS balance, reflecting ANS modulation, are also linked to the gait modulations required for walking on varying inclines (see section 4.5 below).

4.5 | Parasympathetic—Sympathetic Balance During Sensorimotor Integration

As mentioned in the introduction, the contribution of the parasympathetic branch is only part of ANS regulation, as it works in synergy with the sympathetic branch to control the HR (Goldberger 1991). PNS-SNS balance is not uniaxial, that is extending from parasympathetic to sympathetic control, as was presumed in the past (Berntson et al. 1991). Instead, the SNS and the PNS are independently regulated, creating a two-dimensional state space with four joint ANS action modes in which they are either negatively correlated that is spanning from (a) reciprocity-SNS control to (b) reciprocity-PNS control, or positively correlated, that is ranging from (c) coactivation to (d) co-inhibition (Figure 7; left panel). The ability to engage in different activity patterns may allow for flexible modulation of cardiac activity to meet diverse environmental demands (Weissman and Mendes 2021). With this in mind, we can speculate on the results we obtained when we organized RMSSD and SDNN in this two-dimensional autonomic space for each TM incline separately (i.e., level, uphill and downhill), depicting the positioning of the different behavioral periods investigated in this study (i.e., congruent, incongruent IP and incongruent SR; see Figure 7). Within level walking conditions, which entail relatively low levels of physical effort (recall participants were instructed to walk at a natural pace), all values were positioned on the nonreciprocal diagonal. This vector, representing positively correlated sympathetic and parasympathetic activity, is modeled as forming a smaller reservoir of possible action modes, consequently triggering a moderate alteration in HR control (Berntson et al. 1991, 2008). This is in accordance with the moderate effort level required in level walking conditions. In these conditions, we can nicely observe the differential effect exerted by congruent versus incongruent periods on SNS-PNS activity. Specifically, the congruent periods seem to trigger SNS–PNS coactivation, suggesting optimal functionality. However, when experiencing sensorimotor incongruence, we observe a shift toward a co-inhibition mode of the two systems, reflecting suboptimal ANS functioning. We suggest this can be a result of the added mental stress this period is entailing due to the conflicting sensorial cues (see Figure 7). A similar trend was observed in the results of the downhill walking conditions, which share the same overall minimal physical effort as level walking conditions. Additionally, in both level and downhill walking, the latter incongruent SR period demonstrates the recovery phase toward congruent ANS mode that is correction of current precept via sensorial recalibration, which leads to a change in ANS stimulus. In accordance with the overall quicker response in downhill walking, a full return to baseline is achieved, while at the end of the SR period of level walking, the ANS mode suggests still co-inhibition, that is prolonged recalibration period.

When looking at uphill walking conditions, which entail greater physical exertion and metabolic input, we can observe that all the values are positioned on the reciprocity diagonal (see Figure 7). The negatively correlated activity of the PNS and SNS is modeled as forming a larger reservoir of possible action modes, consequently triggering larger potential changes in HR control (i.e., greater flexibility). This is in accordance with the higher physical effort required in the uphill walking conditions, that is leading to enhanced SNS activity. And indeed, in congruent periods we observe SNS control, allowing for the highest increase of HR according to the demanding task (uphill walking). In contrast, when experiencing sensorimotor incongruence, the control is of the PNS, indicating a sub-optimal ANS mode, again caused by the conflicted sensorial cues. Similarly to level and downhill walking conditions, the latter incongruent SR period in uphill walking demonstrates the recovery phase toward the congruent ANS state; although, also here, not reaching baseline values, that is prolonged recalibration period.

We present here evidence of differential ANS activations that were specifically aligned with the anticipated physical demands of upcoming walking task transitions (e.g., transitioning to up or down inclines or staying in level position; see Figure 5). These findings strengthen our speculation that ANS adjustments are linked to forthcoming gait behavior modifications rather than solely reflecting incongruent information processing. This bottom-up regulatory mechanism facilitates stability restoration through flexible reallocation of internal resources.

5 | Conclusion

We laid behavioral and physiological evidence for the involvement of the ANS in locomotion regulation, by linking changes in the perception of gravity to alterations in HR and HRV, during sensory incongruent circumstances. These findings contribute to the delineation of integrative perception–action processes across all functional domains (e.g., motor control, cognition, affect, and sensory functions) that give rise to human behavior. After demonstrating the sensitivity of ANS function to sensorimotor manipulation, and while circumstances of visual conflict are limited in day-to-day life (restricted ecological validity), future studies should focus on the influence of cognitive–motor interactions on ANS involvement in locomotion regulation.

Author Contributions

Adi Lustig: conceptualization, writing – original draft, writing – review and editing, visualization, methodology, software, formal analysis, data curation. **Amit Benady:** investigation, writing – review and

editing. **Sharon Gilaie-Dotan:** writing – review and editing, supervision. **Meir Plotnik:** conceptualization, methodology, validation, writing – review and editing, supervision.

Conflicts of Interest

The authors declare no conflicts of interest.

Data Availability Statement

The data that support the findings of this study are available from the corresponding author upon reasonable request.

References

Acharya, U. R., K. P. Joseph, N. Kannathal, C. M. Lim, and J. S. Suri. 2006. "Heart Rate Variability: A Review." *Medical and Biological Engineering and Computing* 44: 1031–1051.

Alameda-Pineda, X., E. Ricci, and N. Sebe. 2019. "Multimodal Behavior Analysis in the Wild: An Introduction." In *Multimodal Behavior Analysis in the Wild*, 1–8. Acdemic Press.

Arakaki, X., R. J. Arechavala, E. H. Choy, et al. 2023. "The Connection Between Heart Rate Variability (HRV), Neurological Health, and Cognition: A Literature Review." *Frontiers in Neuroscience* 17: 1055445.

Assländer, L., and R. J. Peterka. 2016. "Sensory Reweighting Dynamics Following Removal and Addition of Visual and Proprioceptive Cues." *Journal of Neurophysiology* 116: 272–285.

Balestrucci, P., E. Daprati, F. Lacquaniti, and V. Maffei. 2017. "Effects of Visual Motion Consistent or Inconsistent With Gravity on Postural Sway." *Experimental Brain Research* 235: 1999–2010.

Benady, A., S. Zadik, O. Ben-Gal, et al. 2021. "Vision Affects Gait Speed but Not Patterns of Muscle Activation During Inclined Walking—A Virtual Reality Study." *Frontiers in Bioengineering and Biotechnology* 9: 127. https://doi.org/10.3389/fbioe.2021.632594.

Benady, A., S. Zadik, G. Zeilig, S. Gilaie-Dotan, and M. Plotnik. 2021. "Gait Speed Modulations Are Proportional to Grades of Virtual Visual Slopes—A Virtual Reality Study." *Frontiers in Neurology* 12: 1366.

Benarroch, E. E. 1993. "The Central Autonomic Network: Functional Organization, Dysfunction, and Perspective." *Mayo Clinic Proceedings* 68: 988–1001.

Berntson, G. G., J. T. Cacioppo, and K. S. Quigley. 1991. "Autonomic Determinism: The Modes of Autonomic Control, the Doctrine of Autonomic Space, and the Laws of Autonomic Constraint." *Psychological Review* 98: 459–487.

Berntson, G. G., G. J. Norman, L. C. Hawkley, and J. T. Cacioppo. 2008. "Cardiac Autonomic Balance Versus Cardiac Regulatory Capacity." *Psychophysiology* 45: 643–652.

Campos, J. L., J. S. Butler, and H. H. Bülthoff. 2014. "Contributions of Visual and Proprioceptive Information to Travelled Distance Estimation During Changing Sensory Congruencies." *Experimental Brain Research* 232: 3277–3289.

Cano Porras, D., G. Zeilig, G. M. Doniger, Y. Bahat, R. Inzelberg, and M. Plotnik. 2020. "Seeing Gravity: Gait Adaptations to Visual and Physical Inclines – A Virtual Reality Study." *Frontiers in Neuroscience* 13: 1308.

Cavagna, G. A., P. A. Willems, and N. C. Heglund. 2000. "The Role of Gravity in Human Walking: Pendular Energy Exchange, External Work and Optimal Speed." *Journal of Physiology* 528, no. 3: 657–668. https://doi.org/10.1111/j.1469-7793.2000.00657.x.

Critchley, H. D., and S. N. Garfinkel. 2015. "Interactions Between Visceral Afferent Signaling and Stimulus Processing." *Frontiers in Neuroscience* 9: 286.

Critchley, H. D., and N. A. Harrison. 2013. "Visceral Influences on Brain and Behavior." *Neuron* 77: 624–638.

De Kloet, R., M. Oitzl, and M. Joëls. 1999. "Stress and Cognition: Are Corticosteroids Good or Bad Guys?" *Trends in Neurosciences* 22: 422–426.

Dionne, I. J., M. D. White, and A. Tremblay. 2002. "The Reproducibility of Power Spectrum Analysis of Heart Rate Variability Before and After a Standardized Meal." *Physiology & Behavior* 75: 267–270.

Dobrushina, O. R., G. A. Arina, L. A. Dobrynina, et al. 2021. "Sensory Integration in Interoception: Interplay Between Top-Down and Bottom-Up Processing." *Cortex* 144: 185–197.

Elor, A., and S. Kurniawan. 2020. "The Ultimate Display for Physical Rehabilitation: A Bridging Review on Immersive Virtual Reality." *Frontiers in Virtual Reality* 1: 595993.

Faul, F., E. Erdfelder, A. G. Lang, and A. G. Buchner. 2007. "Power 3: A Flexible Statistical Power Analysis Program for the Social, Behavioral, and Biomedical Sciences." *Behavior Research Methods* 39: 175–191.

Forte, G., G. Troisi, M. Pazzaglia, V. De Pascalis, and M. Casagrande. 2022. "Heart Rate Variability and Pain: A Systematic Review." *Brain Sciences* 12: 153.

Goldberger, A. L. 1991. "Is the Normal Heartbeat Chaotic or Homeostatic?" *News in Physiological Sciences: An International Journal of Physiology Produced Jointly by the International Union of Physiological Sciences and the American Physiological Society* 6: 87–91.

Hagemann, D., S. R. Waldstein, and J. F. Thayer. 2003. "Central and Autonomic Nervous System Integration in Emotion." *Brain and Cognition* 52: 79–87.

Holzman, J. B., and D. J. Bridgett. 2017. "Heart Rate Variability Indices as Bio-Markers of Top-Down Self-Regulatory Mechanisms: A Meta-Analytic Review." *Neuroscience and Biobehavioral Reviews* 74: 233–255.

Huang, Y., and R. P. N. Rao. 2011. "Predictive Coding." *Wiley Interdisciplinary Reviews: Cognitive Science* 2: 580–593.

Kimel-Naor, S., A. Gottlieb, and M. Plotnik. 2017. "The Effect of Uphill and Downhill Walking on Gait Parameters: A Self-Paced Treadmill Study." *Journal of Biomechanics* 60: 142–149.

Kleiger, R. E., P. K. Stein, and J. T. Bigger. 2005. "Heart Rate Variability: Measurement and Clinical Utility." *Annals of Noninvasive Electrocardiology* 10: 88–101.

Laborde, S., E. Mosley, and J. F. Thayer. 2017. "Heart Rate Variability and Cardiac Vagal Tone in Psychophysiological Research - Recommendations for Experiment Planning, Data Analysis, and Data Reporting." *Frontiers in Psychology* 8: 213. https://doi.org/10.3389/fpsyg.2017.00213.

Lacquaniti, F., G. Bosco, S. Gravano, et al. 2014. "Multisensory Integration and Internal Models for Sensing Gravity Effects in Primates." *BioMed Research International* 2014: 1–10.

Lacquaniti, F., G. Bosco, S. Gravano, et al. 2015. "Gravity in the Brain as a Reference for Space and Time Perception." *Multisensory Research* 28: 397–426.

Larra, M. F., J. B. Finke, E. Wascher, and H. Schächinger. 2020. "Disentangling Sensorimotor and Cognitive Cardioafferent Effects: A Cardiac-Cycle-Time Study on Spatial Stimulus-Response Compatibility." *Scientific Reports* 10: 4059.

Larsen, P. D., Y. C. Tzeng, P. Y. W. Sin, and D. C. Galletly. 2010. "Respiratory Sinus Arrhythmia in Conscious Humans During Spontaneous Respiration." *Respiratory Physiology & Neurobiology* 174: 111–118.

Malik, M., J. T. Bigger, A. J. Camm, et al. 1996. "Heart Rate Variability. Standards of Measurement, Physiological Interpretation, and Clinical Use." *European Heart Journal* 17: 354–381.

McCraty, R., and F. Shaffer. 2015. "Heart Rate Variability: New Perspectives on Physiological Mechanisms, Assessment of Self-Regulatory Capacity, and Health Risk." *Global Advances in Health and Medicine* 4: 46–61.

McEwen, B. S. 1998. "Protective and Damaging Effects of Stress Mediators." *New England Journal of Medicine* 338: 171–179.

Minetti, A. E., C. Moia, G. S. Roi, D. Susta, and G. Ferretti. 2002. "Energy Cost of Walking and Running at Extreme Uphill and Downhill Slopes." *Journal of Applied Physiology* 93: 1039–1046.

Munoz, L. M., A. van Roon, H. Riese, et al. 2015. "Validity of (Ultra-) Short Recordings for Heart Rate Variability Measurements." *PLoS One* 10, no. 9: e0138921.

O'Connor, S. M., and J. M. Donelan. 2012. "Fast Visual Prediction and Slow Optimization of Preferred Walking Speed." *Journal of Neurophysiology* 107: 2549–2559.

Ottaviani, C. 2018. "Brain-Heart Interaction in Perseverative Cognition." *Psychophysiology* 55: e13082.

Owens, A. P. 2020. "The Role of Heart Rate Variability in the Future of Remote Digital Biomarkers." *Frontiers in Neuroscience* 14: 1–10.

Owens, A. P., M. Allen, S. Ondobaka, and K. J. Friston. 2018. "Interoceptive Inference: From Computational Neuroscience to Clinic." *Neuroscience and Biobehavioral Reviews* 90: 174–183.

Owens, A. P., K. J. Friston, D. A. Low, C. J. Mathias, and H. D. Critchley. 2018. "Investigating the Relationship Between Cardiac Interoception and Autonomic Cardiac Control Using a Predictive Coding Framework." *Autonomic Neuroscience: Basic & Clinical* 210: 65–71.

Pearson, K. G. 2004. "Generating the Walking Gait: Role of Sensory Feedback." *Progress in Brain Research* 143: 123–129.

Plotnik, M., T. Azrad, M. Bondi, et al. 2015. "Self-Selected Gait Speed - Over Ground Versus Self-Paced Treadmill Walking, a Solution for a Paradox." *Journal of Neuroengineering and Rehabilitation* 12: 20.

Rodrigues, J., E. Studer, S. Streuber, N. Meyer, and C. Sandi. 2020. "Locomotion in Virtual Environments Predicts Cardiovascular Responsiveness to Subsequent Stressful Challenges." *Nature Communications* 11: 5904.

Salahuddin, L., J. Cho, M. G. Jeong, and D. Kim. 2007. "Ultra Short Term Analysis of Heart Rate Variability for Monitoring Mental Stress in Mobile Settings." Annual International Conference of the IEEE Engineering in Medicine and Biology–Proceedings, 4656–4659. https://doi.org/10.1109/IEMBS.2007.4353378.

Shaffer, F., and J. P. Ginsberg. 2017. "An Overview of Heart Rate Variability Metrics and Norms." *Frontiers in Public Health* 5: 258.

Skaggs, S. 2023. "References and Notes." *Hidden Factor* 314: 170–171.

Smith, R., J. F. Thayer, S. S. Khalsa, and R. D. Lane. 2017. "The Hierarchical Basis of Neurovisceral Integration." *Neuroscience and Biobehavioral Reviews* 75: 274–296.

Smith, T. W., C. Deits-Lebehn, P. G. Williams, B. R. W. Baucom, and B. N. Uchino. 2020. "Toward a Social Psychophysiology of Vagally Mediated Heart Rate Variability: Concepts and Methods in Self-Regulation, Emotion, and Interpersonal Processes." *Social and Personality Psychology Compass* 14: e12516.

Soares-Miranda, L., J. Sattelmair, P. Chaves, et al. 2014. "Physical Activity and Heart Rate Variability in Older Adults: The Cardiovascular Health Study." *Circulation* 129: 2100–2110.

Thayer, J. F., F. Åhs, M. Fredrikson, J. J. Sollers, and T. D. Wager. 2012. "A Meta-Analysis of Heart Rate Variability and Neuroimaging Studies: Implications for Heart Rate Variability as a Marker of Stress and Health." *Neuroscience and Biobehavioral Reviews* 36: 747–756.

Thayer, J. F., A. L. Hansen, E. Saus-Rose, and B. H. Johnsen. 2009. "Heart Rate Variability, Prefrontal Neural Function, and Cognitive Performance: The Neurovisceral Integration Perspective on Self-Regulation, Adaptation, and Health." *Annals of Behavioral Medicine* 37: 141–153.

Thayer, J. F., and E. Sternberg. 2006. *Beyond Heart Rate Variability: Vagal Regulation of Allostatic Systems*, 361–372. Annals of the New York Academy of Sciences, (Blackwell Publishing Inc.).

Thayer, J. F., S. S. Yamamoto, and J. F. Brosschot. 2010. "The Relationship of Autonomic Imbalance, Heart Rate Variability and Cardiovascular Disease Risk Factors." *International Journal of Cardiology* 141: 122–131.

Weissman, D. G., and W. B. Mendes. 2021. "Correlation of Sympathetic and Parasympathetic Nervous System Activity During Rest and Acute Stress Tasks." *International Journal of Psychophysiology* 162: 60–68.

Supporting Information

Additional supporting information can be found online in the Supporting Information section.